ADVANCED FUNCTIONAL MATERIALS
www.afm-journal.de

www.MaterialsViews.com

Dendron-Based Micelles for Topical Delivery of Endoxifen: A Potential Chemo-Preventive Medicine for Breast Cancer

*Yang Yang, Ryan M. Pearson, Oukseub Lee, Chan-Woo Lee, Robert T. Chatterton Jr., Seema A. Khan, and Seungpyo Hong**

Endoxifen (EDX) is an active metabolite of tamoxifen that has been proven effective in the prevention and treatment of estrogen-positive breast cancer; however, oral administration of tamoxifen often causes severe side effects. Here, the topical delivery of EDX is explored using polymeric micelles to achieve localized drug delivery with potentially minimal side effects. EDX is encapsulated into dendron micelles (DM) with various surface groups (-NH_2, -COOH, or -Ac) and into cationic liposomes as a control. End-group modification significantly affects the drug loading, where the DM-COOH micelles allow the most efficient encapsulation. Furthermore, unlike the burst release from the liposomes, all DMs show sustained release of EDX over 6 days. Each formulation is evaluated for its potential to deliver EDX across the skin layers. DMs substantially enhance the permeation of EDX through both mouse (up to 20-fold) and human (up to 4-fold) skin samples relative to ethanol, a chemical penetration enhancer. Franz diffusion cell experiments reveal that DM-COOH induces the highest flux of EDX among all groups. The enhanced drug loading, controlled release profiles, and enhanced skin permeation all demonstrate that DMs are a useful platform for the topical delivery of EDX, offering a potential alternative administration route for chemoprevention.

1. Introduction

Endoxifen (4-hydroxy-*N*-desmethyl tamoxifen, or EDX) is the primary metabolite of tamoxifen and is known to be responsible for the overall effectiveness of tamoxifen against estrogen receptor-positive (ER+) breast cancer.[1] The conversion of tamoxifen to its active form EDX is dependent on the activities of cytochrome P450 isoforms (e.g. CYP2D6 and CYP3A4/5).[1,2] Although controversial,[3] women with genetically impaired CYP2D6 activity (homozygous for two null CYP2D6) have been reported to have a higher propensity for breast cancer recurrence with tamoxifen treatment,[1] a concern which also applies to the prevention setting. Thus, direct administration of EDX to the breast through its skin envelope could potentially avert the problem of inefficient metabolism of tamoxifen.[4] Furthermore, local transdermal delivery to the breast should decrease side effects[4] such as hot flashes, vaginal atrophy, higher risk of endometrial cancer and thromboembolic events, which are the collateral damage of systemic exposure to tamoxifen.[5–7] Therefore, a localized, topical EDX delivery system to the breast would offer a promising alternative way to minimize its systemic exposure,[8] which could potentially reduce the side effects observed from conventional oral tamoxifen/EDX treatment and help women with impaired CYP2D6 activities.

For EDX to be effectively delivered through the skin layers, it must traverse through multiple barriers. In particular, the stratum corneum (SC), the topmost skin layer, is the most significant barrier that needs to be overcome to effectively deliver drugs across the skin layers.[9] EDX is a relatively hydrophobic small molecule with an octanol-water partition coefficient (log*P*) above 4.0.[10] As this log*P* value is beyond the optimum range (between 1 and 3) for efficient skin permeation,[11–15] EDX alone cannot effectively pass through the skin layers without the use of penetration enhancers.[16]

Chemical penetration enhancers (CPEs), such as ethanol and sodium dodecyl sulfate (SDS), have been commonly used to enhance the skin permeability of therapeutic molecules that are otherwise skin impermeable.[13] However, significant irritation and adverse effects have been often observed because of skin dehydration and/or SC lipid disruption, which is proportional to the penetration enhancement abilities of the individual CPE.[13,17] To overcome the problem of skin irritation, a number of polymeric penetration enhancers have been introduced as potential platforms for transdermal drug delivery.[18–22]

Dr. Y. Yang, R. M. Pearson, Dr. S. Hong
Department of Biopharmaceutical Sciences
College of Pharmacy
University of Illinois
Chicago, IL, 60612, USA
E-mail: sphong@uic.edu
Dr. O. Lee, Dr. S. A. Khan
Department of Surgery
Robert H. Lurie Comprehensive Cancer Center
Feinberg School of Medicine
Northwestern University
Chicago, IL, 60611, USA
C.-W. Lee
Research and Development Center
Durae Co., Gunpo, Gyeonggi-do, Republic of Korea
Dr. R. T. Chatterton, Jr.
Department of Obstetrics/Gynecology
Robert H. Lurie Comprehensive Cancer Center
Feinberg School of Medicine
Northwestern University
Chicago, IL, 60611, USA

DOI: 10.1002/adfm.201303253

In our previous study, skin interactions of polyamidoamine (PAMAM) dendrimers were investigated.[11] We reported that skin permeation and retention behaviors of PAMAM dendrimers can be significantly modulated by surface engineering, which is likely due to the high density surface groups of dendrimers. Surface-modification by acetylation or carboxylation produced an enhancement of skin permeation of dendrimers. However, drug delivery using dendrimers has limitations, since the preferred method to stably carry drug molecules for dendrimers is through chemical conjugation that could also result in decreased drug efficacy.[23] The lack of a highly reactive functional group on EDX further limits the use of dendrimers for this particular drug molecule.

To take advantage of the dendritic structure for significant surface group effect while maintaining the efficacy of hydrophobic drugs, we have recently developed biocompatible, amphiphilic PEGylated dendron-based copolymers (PDCs) that are a hybridization of dendritic structure and linear-block copolymers.[24] In aqueous environment, PDCs self-assemble into dendron micelles (DMs) that can efficiently encapsulate hydrophobic molecules into the core (**Figure 1**). The low critical micelle concentrations (CMCs) of the DMs (on the order of 10^{-8} M)[24,25] demonstrate their remarkable thermodynamic stability for hydrophobic drug delivery. Additionally, the hyperbranched dendrons confer similar properties of dendrimers to the DM, such as high-density peripheral functional groups and ease of surface functionalization.[23,24]

Considering all of these above, we hypothesized that the DMs would achieve sufficient loading, enhanced skin permeation, and controlled release profile of EDX without a cost of its efficacy, compared to free EDX. To test this hypothesis, we encapsulated EDX into the DMs and compared its skin permeation to those formulated with cationic liposomes and a traditional CPE (ethanol) using both hairless mouse and human skin samples. By modulating the end-group functionalities of the DMs, the surface charge effect on drug loading, in vitro drug release, and skin permeation were also systematically studied. Our data indicate that the DMs have great potential as a novel platform for controlled topical delivery of EDX.

2. Results and Discussion

A DM platform was developed to achieve effective EDX encapsulation and delivery via topical administration. PDCs were synthesized from the combination of a single hydrophobic core-forming block poly-ε-caprolactone (PCL) with multiple hydrophilic poly(ethylene glycol) (PEG) chains mediated by a generation 3 (G3) polyester dendron.[24,25] Encapsulation of EDX into DMs through self-assembly provided a water-soluble drug formulation and offered the potential to deliver EDX without the use of CPEs, while maintaining the surface functionality of the DMs. In addition to a CPE (ethanol), cationic liposomes were used as a control. 1,2-dioleoyl-3-trimethylammonium-propane (DOTAP) and 1,2-dimyristoyl-sn-glycero-3-phosphocholine (DMPC) were chosen as lipid components to respectively provide cationic charges and liquid crystalline phase to the liposomes, which are known to enhance skin permeability.[26,27]

The particle size, zeta potential, and drug loading values of various formulations used in this study are listed in **Table 1**. The encapsulation of EDX into DMs yielded number-weighted average diameters between 40 and 50 nm with a narrow size distribution, which were in agreement with images obtained using transmission electron microscopy (TEM) (Figure 1A–C). In contrast, EDX-loaded liposomes employed as a control group had an average size of 100 nm in diameter. The smaller size of DMs resulted in a larger surface-area-to-volume ratio, which would facilitate better interaction with the skin surface.[13] The zeta potential measurements revealed that amine-terminated dendron micelles (denoted as DM-NH_2) and liposomes were

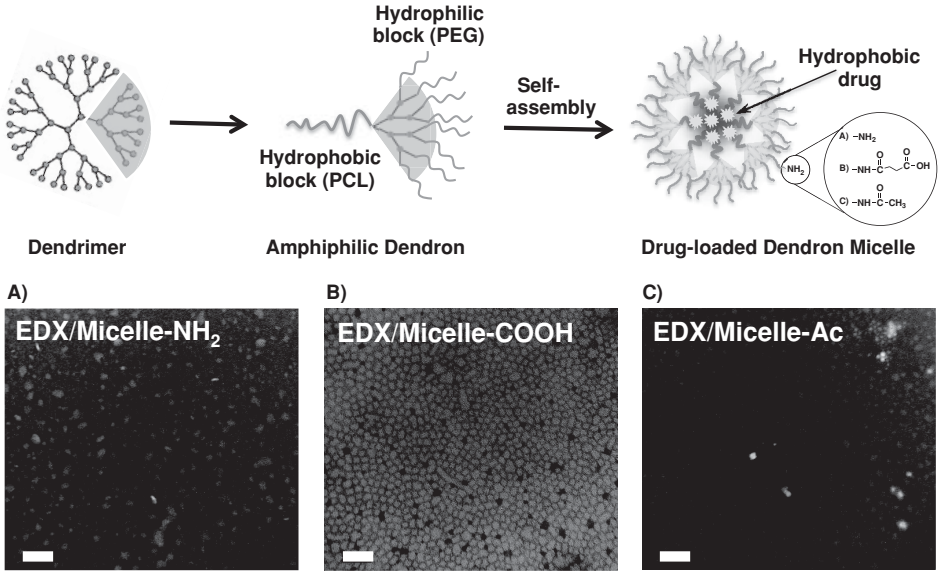

Figure 1. Schematics of the PEGylated dendron-based copolymer (PDC, top panel) and morphology (TEM images, bottom panel) of EDX-loaded dendron micelles (DMs) with A) amine, B) carboxyl, or C) acetamide surface groups. Scale bars: 100 nm.

Table 1. Characterization of EDX-loaded dendron micelles and liposomes.

Materials	Size [nm][a)]	ζ-Potential [mV]	Drug Loading[b)]	Loading [%][c)]	EE [%][d)]
EDX/DM-NH_2	48.7 ± 7.1	42.9 ± 1.6	3.0 ± 1.3	0.3 ± 0.1%	2.0 ± 0.9%
EDX/DM-Ac	37.4 ± 6.2	-2.7 ± 1.4	5.7 ± 0.2	0.6 ± 0.0%	3.8 ± 0.1%
EDX/DM-COOH	48.4 ± 6.1	-23.2 ± 3.5	29.7 ± 2.0	3.0 ± 0.2%	19.8 ± 1.4%
EDX/Liposome	100.5 ± 20.9	28.6 ± 0.3	0.4 ± 0.0	0.1 ± 0.1%	0.0 ± 0.0%
Cou-6/DM-RHO-NH_2	75.2 ± 8.3	–	1.2 ± 0.1	0.1 ± 0.0%	6.1 ± 0.7%
Cou-6/DM-RHO-Ac	24.0 ± 4.2	–	1.6 ± 0.2	0.1 ± 0.0%	8.2 ± 1.1%
Cou-6/DM-RHO-COOH	24.5 ± 3.3	–	1.2 ± 0.1	0.1 ± 0.0%	6.2 ± 0.7%

[a)]Measured using dynamic light scattering (DLS); [b)]Measured using RP-HPLC, expressed as "μg of drug / mg of DMs"; [c)]$Loading\% = \frac{Total\ amount\ of\ drug\ encapsulated\ (\mu g)}{Total\ weight\ of\ nanoparticles\ (\mu g)} \times 100\%$
[d)]$EE\%,\ Encapsulation\ Efficiency\% = \frac{Amount\ of\ drug\ encapsulated\ (\mu g)}{Amount\ of\ drug\ added\ for\ encapsulation\ (\mu g)} \times 100\%$ All data presented are mean ± SD.

positively charged (42.9 ± 1.6 mV and 28.6 ± 0.3 mV, respectively) when measured in ddH_2O (pH 5.6). Following surface modification, the surface charge of acetamide-terminated micelles (denoted as DM-Ac) was decreased to nearly neutral (–2.7 ± 1.4 mV), and that of carboxyl-terminated micelles (denoted as DM-COOH) was reversed to a negative value (–23.2 ± 3.5 mV). Drug loading measurements revealed that liposomes encapsulated the least amount of EDX (0.4 ± 0.0 μg/mg liposome), likely due to their aqueous core and smaller hydrophobic regions than DMs, which hindered effective encapsulation of hydrophobic molecules.[28] Interestingly, DM-COOH encapsulated the highest amount of EDX (29.7 ± 2.0 μg/mg DM-COOH, almost 75-fold higher than in liposome). DM-NH_2 and DM-Ac demonstrated relatively modest drug loading of 3.0 ± 1.3 μg/mg and 5.7 ± 0.2 μg/mg, respectively.

The substantially higher EDX loading of DM-COOH may be at least partially explained by the ion-pairing phenomenon. According to Turco Liveri et al.,[29] hydrophobic drug molecules encapsulate into the core of micelles through three steps of aqueous, hydrophilic corona, and hydrophobic core pseudophases. For our micelle preparation, the drug partition at the aqueous pseudophase would be important during the encapsulation process using dialysis where initial interactions occur between drug molecules and the surface groups of the micelles. As a result, differently charged surface groups may be responsible for the observation of distinctly different EDX loading of the DMs. Depending on the pKa of the drug encapsulated and pH of the aqueous solvent, ion pairing between the surface groups and the drug molecules may occur, inducing drug loading thermodynamically favorable. In the case of DM-COOH, EDX with an estimated pKa above 9.0 (estimated using physico-chemical property predictors, ChemAxon, Cambridge, MA) will be positively charged at neutral pH, whereas the carboxyl group of DM-COOH will be negatively charged based on the zeta potential measurement, facilitating the formation of ion pairs.

Next, the release profiles of EDX from the DMs and liposomes were monitored. As shown in **Figure 2**, cationic liposomes completely released the encapsulated EDX within 8 h at the fastest release rate of 9.47%/h, indicating that the liposomes are unable to stably encapsulate EDX. In contrast, release of EDX from the surface-modified DMs occurred in a controlled manner following a biphasic release profile. During the initial 8 h, the release rate of EDX followed the order of DM-COOH (8.38%/h, 71.4% total release), DM-Ac (6.36%/h, 59.7%

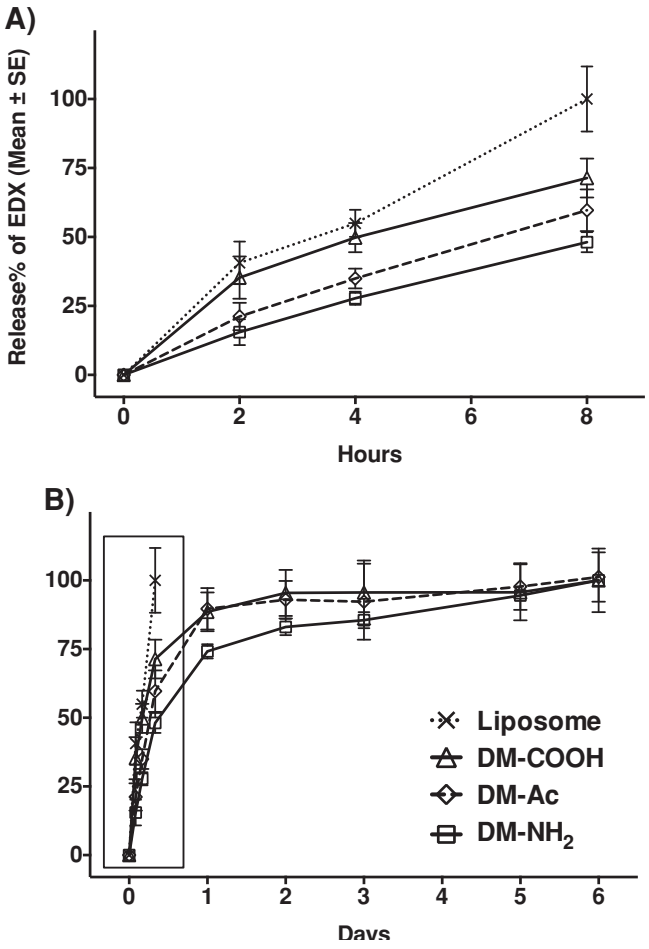

Figure 2. In vitro EDX release from liposomes and surface modified DMs. A) Release profiles of EDX from various formulations over the first 8 h. Note that the liposomes reached 100% release of EDX only after 8 h. B) Release profiles of EDX from the DMs over an extended period of time (6 days). Error bars: standard error (SE, n = 3).

total release), and DM-NH_2 (5.62%/h, 48.1% total release). The release of EDX appeared to be surface charge-dependent. When applied with the same initial dose based on EDX, DM-COOH with the highest drug loading exhibited the fastest drug release, whereas DM-NH_2 had the lowest drug loading and the slowest release rate among the three DMs. This early, fast drug release could be attributed to the presence of EDX molecules adsorbed on the DM surfaces during the micelle preparation process.[30] The remaining EDX was then released slowly and steadily from the DMs over 144 h (6 days). For this second phase, the release rate followed the order of DM-NH_2 (0.20%/h), DM-Ac (0.08%/h), and DM-COOH (0.07%/h). This prolonged release of EDX by DMs is particularly important because this drug delivery system is intended to provide a potential tool for chemoprevention. Given that the target recipients are those who have potential to develop breast cancer, a slow release system could reduce dosing frequency, which would significantly increase the patient compliance.

To ensure that EDX maintains its ER-dependent anti-proliferative effect after encapsulation into three types of surface-modified DMs, MTS assays were performed on ER+ MCF-7 and ER-negative (ER–) MDA-MB-231 breast cancer cells. Compared to the β-estradiol (E2)-treated groups (checkered bars), addition of free EDX (solid black bars) exhibited concentration-dependent growth inhibition against MCF-7 cells (**Figure 3** and Figure S1 in the Supporting Information (SI)). As observed on days 5, 8, and 12 after treatments, DM-loaded EDX applied at the same concentration as free EDX demonstrated comparable efficacy without distinction of the surface functionalities of the DMs (Figure 3 and Figure S1 in the SI). In contrast, neither the EDX-loaded DMs nor free EDX demonstrated anti-proliferative effect against ER– MDA-MB-231 cells (Figure S2 in the SI). Additionally, the surface-modified empty DMs did not cause significant cytotoxicity towards MCF-7 cells at a concentration up to 1 μM (Figure S3 in the SI), which is in agreement with our previous report where concentrations of surface modified empty DMs were non-toxic to KB cells at concentrations up to 100 μM.[25] These results indicate that the observed growth inhibition of MCF-7 cells is due to the fact that EDX maintains its ER-specific anti-proliferative efficiency after encapsulation, and that the EDX-loaded DMs are non-toxic, suitable for delivery of chemo-preventive medicine.

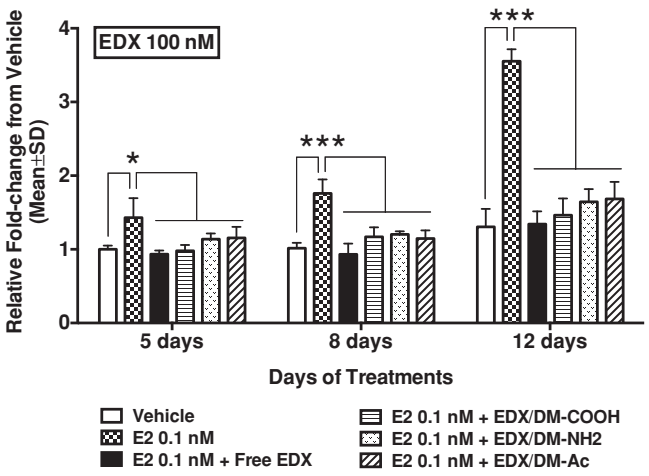

Figure 3. In vitro anti-proliferative effect of EDX in its free from and in surface-modified DMs on MCF-7 cells evaluated using MTS assay. The anti-proliferative effect of EDX encapsulated into DMs is comparable to that of free EDX. All groups were treated with 0.1 nM of E2 (β-estradiol) except for the vehicle group (0.01% DMSO). Error bars: standard deviation, SD, n = 3. *$p < 0.05$; ***$p < 0.001$.

We then compared our DM systems with CPEs and cationic liposomes, which have been commonly used for transdermal drug delivery,[26,31–33] in terms of skin permeation and retention. The skin permeation parameters of EDX in various formulations used in this study are summarized in **Table 2**. Using hairless mouse skin, we observed that the rate of EDX permeation (flux) was proportional to drug loading, i.e., DM-COOH was significantly greater than DM-Ac, DM-NH_2, and liposomes with the flux values of 155, 67, 45, and 44 ng/cm^2/h, respectively (Table 2 and **Figure 4**A). A larger permeability coefficient (K_p) of 4.7×10^{-2} cm/h was obtained from the liposomes compared to the DMs. All nanomaterials shortened the lag time for EDX to reach the steady permeation through the skin layers, compared to ethanol. The diffusion coefficients (D) were similar throughout all formulations, indicating that the mouse skin samples used in this study had similar integrities and thickness. Enhancement ratios (ER) were calculated to show the enhancement in flux in a clear manner, which revealed that

Table 2. Skin permeation parameters of EDX delivered through mouse and human skin.

Skin type	Vehicles	Flux (J) [ng/cm^2/h]	Lag time [h]	Permeability Coefficient (K_p) [cm/h]	Diffusion Coefficient (D) [cm^2/h]	Enhancement Ratio (ER)
Mouse	EtOH	17.1	11.0	4.6×10^{-4}	6.1×10^{-6}	1.0
	Liposome	44.1	8.3	46.7×10^{-3}	8.0×10^{-6}	2.6
	DM-NH_2	45.0	9.0	79.5×10^{-4}	7.4×10^{-6}	2.6
	DM-Ac	66.5	9.8	91.7×10^{-4}	6.8×10^{-6}	3.9
	DM-COOH	154.7	9.9	37.9×10^{-4}	6.8×10^{-6}	9.0
Human	EtOH	7.5	12.3	6.7×10^{-4}	2.0×10^{-5}	1.0
	EtOH w/ OA	14.7	11.7	13.3×10^{-4}	2.2×10^{-5}	2.0
	DM-COOH	30.2	11.4	27.3×10^{-4}	2.2×10^{-5}	4.0

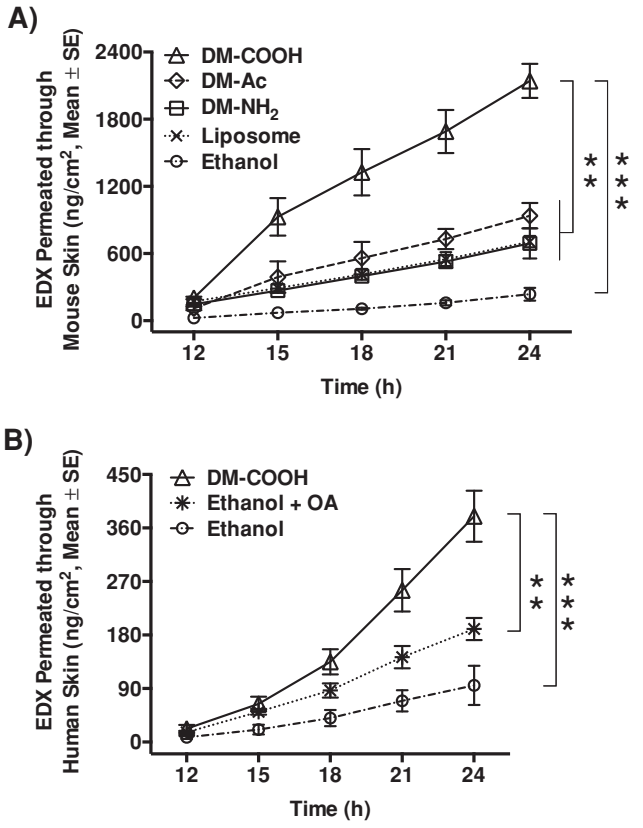

Figure 4. Skin permeation of EDX delivered by various vehicles across mouse and human skin. A) Mouse skin permeation of EDX over 24 h. B) Human skin permeation of EDX over 24 h. DM-COOH induces permeation of the highest amount of EDX across the both mouse and human skin layers. OA, oleic acid. Error bars: standard error, SE, n = 3–6. $^{**}p < 0.005$; $^{***}p < 0.001$.

DM-COOH achieved a 9-fold enhancement compared to ethanol. In general, the high flux, short lag time, and positive *ER* values demonstrate that all nanomaterials used in this study are effective in terms of enhancing EDX to permeate through the skin layers.

Similar to the drug loading, the substantially enhanced *ER* for DM-COOH can be explained by ion pairing. The charge sequestration of EDX by ion pairing may potentially facilitate skin permeation of EDX because charged drug molecules typically cannot partition into or permeate across the skin.[12] Although the highest permeation coefficient was obtained by using liposomes, the poor EDX loading (0.4 μg EDX/mg liposome) necessitates a larger amount of liposomes to deliver the same amount of EDX compared to DMs. Approximately 7.5, 14.3, and 74.3 times more amounts of liposomes would be required to deliver the same amount of EDX, compared to DM-NH_2, DM-Ac, and DM-COOH, respectively. It is likely that liposomes would be a good delivery vehicle for hydrophilic or amphiphilic molecules that can be incorporated into the aqueous core of the liposomes at high efficiency.[34] For highly hydrophobic EDX, however, DM-COOH that achieves the highest drug loading and flux of EDX appears to be the superior drug carrier among the groups tested in this study.

To further validate the efficiency of DM-COOH as a topical delivery system for EDX, we used split-thickness human skin samples. Compared to commonly used CPEs (ethanol and ethanol-oleic acid (OA) combination,[4] DM-COOH showed significantly more efficient skin permeation of EDX across the human skin, as measured by a higher EDX flux, shorter lag time, and greater permeability coefficient (Table 2). As shown in Figure 4B, DM-COOH achieved a substantially increased flux of EDX (30.2 ng/cm^2/h) that is 4-fold and 2-fold higher than 60% ethanol (7.5 ng/cm^2/h) and the ethanol-OA formulations (14.7 ng/cm^2/h) through the human skin, respectively. The obtained skin permeation parameters were lower than those obtained from a previous study using ethanol-OA combination,[4] which is likely due to the lower amount of EDX applied to the human skin in this experiment. The human skin permeation of EDX was lower than mouse skin, probably due to the thickness difference in SC; ~26 μm for human[35] vs. ~15 μm for mouse skin,[36] as confirmed by the longer lag time. Nonetheless, these results assure that the trend observed in the mouse skin is translatable to human skin, demonstrating that DMs, DM-COOH in particular, is a promising topical delivery system for EDX.

To better understand how the DMs facilitate the delivery of small hydrophobic molecules through skin layers, two-dye fluorescent-labeled DMs were also prepared. Coumarin-6 (Cou6) was encapsulated into the core of the micelles and the surface of the micelles was conjugated with rhodamine (RHO). Characterization of these two-dye systems is listed in Table 1 where the diameters of the three DMs varied ranging approximately 25–75 nm and the drug loading values were 1.2–1.6 μg/mg. The CLSM images shown in **Figure 5**A demonstrate the localization of Cou6 in mouse skin after 24 h treatment using the Franz cells. As seen from the green signal of Cou6 in the images, DMs induced high levels of the encapsulated Cou6 to reach both the epidermal and dermal layers. By way of contrast, the lack of green signal in Figure 5B indicates that free Cou6 could not diffuse into the skin layers even in the presence of ethanol. The skin retention of Cou6 was also analyzed using a spectrofluorometer. Figure 5C shows that all three types of micelles delivered significantly higher amounts of Cou6 through the mouse skin (DM-COOH: 67 ± 6%, DM-Ac: 68 ± 2%, and DM-NH_2: 66 ± 4%) than free Cou6 delivered by ethanol (EtOH: 27 ± 3%). However, given the similarity of the drug loading, there was no significant difference among surface modified DMs in depositing the encapsulated Cou6 into the skin layers. This observation indicates that permeation of EDX using the DMs, is directly related to the drug loading. Therefore, it will be important to investigate case-by-case for different drugs in order to have the proper surface groups on the DMs for optimum encapsulation to obtain optimal skin permeation.

As demonstrated above, DMs can efficiently encapsulate and deliver hydrophobic small molecules into the skin layers. According to studies using small molecule-based micelles for topical drug delivery,[18,20,37,38] the mechanism behind this phenomenon could be explained by skin barrier perturbation,[39] but not by skin irritation.[40] As reported by Ghosh et al., the size of the micelle can directly dictate how easily it permeates the skin, thus determining whether it causes skin irritations.[40] They claimed that the skin penetration of micelles was mostly through aqueous porous pathway. The average

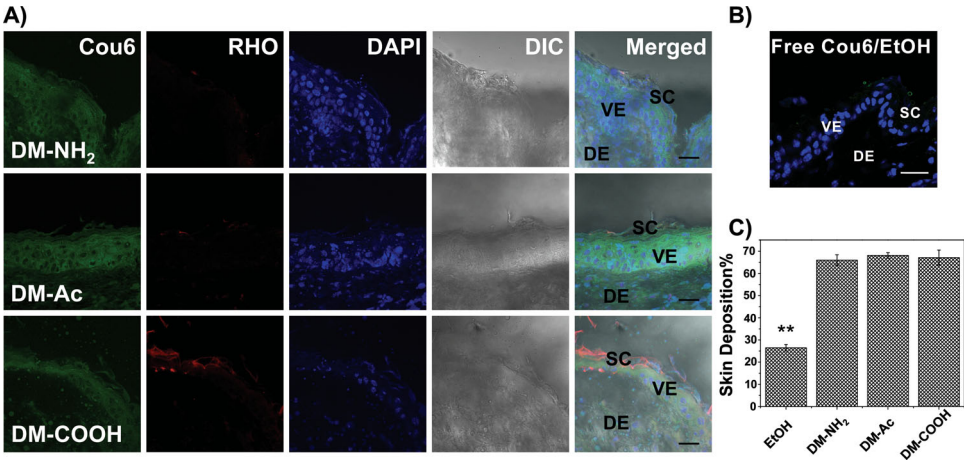

Figure 5. Skin deposition of Cou6-encapsulated, RHO-labeled two-dye DMs. A) Images of the SKH1 hairless mouse skin cross-sections after treatment with DM-NH_2, DM-Ac, or DM-COOH for 24 h. CLSM images in different channels show localization of Cou6 (green), RHO (DM, red), and DAPI (cell nuclei, blue) individually, and are merged with DIC images. Although DMs (red) are not prevalently present in the skin layers, they induce significant skin penetration of Cou6. B) A merged CLSM image of mouse skin cross-section after treatment with free Cou6 in ethanol (EtOH) for 24 h. No green signal is observed, indicating that free Cou6 cannot penetrate the skin layers even in the presence of ethanol. C) Skin deposition of Cou6 delivered by DMs or EtOH, measured using a spectrophotometer after skin extraction with DMSO. SC, stratum corneum; VE, viable epidermis; DE, dermal layer. Scale bars: 20 μm, Error bars: standard error, SE, n = 3. $^{**}p < 0.005$.

size of skin aqueous pores is 2.9 ± 0.5 nm, and the measured radius of SDS micelles was 2.0 ± 0.1 nm. Thus, they could cause skin irritation, whereas the larger micelles (sodium cocoyl isethionate (SCI) micelle with 3.4 ± 0.1 nm radius) did not.[40] In our study, all of the prepared micelles are substantially larger than both SDS and SCI micelles (Table 1); thus, they are not permeable across the skin, as confirmed by CLSM observations of the two-dye micelle system (Figure 5A). However, according to our permeation results, these micelles effectively facilitate skin translocation of Cou6 and EDX despite the fact that the micelles are almost skin impermeable. From the CLSM images (Figure 5A), the permeated dye is not confined to hair follicle regions, which implies that micelles may deliver the encapsulated hydrophobic molecules mainly through free-volume diffusion (through lipid bilayers) and lateral diffusion (along lipid bilayers).[41] Although further studies are required to fully understand the mechanisms of DM-skin interactions, the results presented in this paper clearly demonstrate the potential of DMs for efficient topical delivery of EDX with reduced skin irritation concerns.

3. Conclusion

In this study, we have demonstrated that the DMs can successfully encapsulate EDX, release it in a controlled manner, and enhance its skin permeation into mouse and human skin. The enhanced skin permeation is largely attributed to the high drug loading in the DMs, especially those with carboxyl surface groups. Skin localization studies using the two-dye DMs demonstrated that DMs deliver the encapsulated hydrophobic molecules through the skin without entering the skin layers as a whole, thus skin irritation from the polymers can be potentially avoided. This study presents the potential of DMs as a topical drug delivery platform and also indicates that the DM structures may need to be individually designed depending upon the properties of drug molecules.

4. Experimental Section

Materials: EDX (*N*-desmethyl-4-hydroxy tamoxifen, M_w 373.49, E/Z 1:1 mixture) was purchased from Toronto Research Chemicals Inc. (North York, Ontario, Canada). DOTAP (MW 698.54), DMPC (MW 677.93), and Cholesterol (MW 386.65) were obtained from Avanti Polar Lipids, Inc. (Alabaster, AL). Surface modified PDCs and their respective dendron micelles (denoted as DM-end group) were prepared in house as described previously with the following end-groups (-NH_2, -COOH, and -Ac).[25] Cou6, 17β-estradiol (E2), all solvents for chemical reactions, including dimethylformamide (DMF), dimethyl sulfoxide (DMSO), dichloromethane (DCM) and methanol, and all other chemicals were obtained from Sigma-Aldrich (St. Louis, MO) and used without further purification.

Preparation of EDX-loaded DMs with Different Surface Functional Groups: EDX-loaded DMs were prepared using a dialysis method as described in our earlier publications.[25] Briefly, 10 milligrams of the surface modified PDC were dissolved in 1 mL (10 mg/mL) of DMF along with 1.5 mg of EDX. The polymer-EDX mixture was then transferred to a dialysis membrane (MWCO 3500) and dialyzed for 24 h against 500 mL of double distilled water (ddH_2O). After dialysis, the micelle solution was collected into 1.5 mL centrifuge tubes and centrifuged at 10 000 rpm for 5 min at 25 °C. The supernatant was carefully collected and freeze-dried for 2 days to obtain the EDX-loaded DM. Methods of characterizations including morphology observations and drug loading measurements are described in the SI.

Preparation of EDX-loaded Cationic Liposomes: EDX-loaded liposomes were prepared by a thin film hydration method.[32] DOTAP (4.5 mg), DMPC (4.3 mg), Cholesterol (1.2 mg) (2:2:1 molar ratio), and EDX (1.5 mg) were dissolved in 1 mL of chloroform. The solvent was evaporated using a rotary evaporator until the materials formed a thin, dried film at the bottom of the round-bottom flask. Two milliliters of ddH_2O were added to rehydrate (completely re-dissolve) the lipid film by vortexing at high intensity. The rehydrated materials were then sonicated for 30–60 min in a water bath sonicator. The size of the liposome was further refined by extrusion 40 times through a polycarbonate membrane (pore size 100 nm)

at 40 psi. The liposomes prepared were then collected into 1.5 mL centrifuge tubes and centrifuged at 13 000 rpm for 30 min at 4 °C. The supernatant was carefully collected and stored in a separate tube for characterization. The liposome pellet was re-suspended in 1 mL of 5% sucrose/water solution, followed by lyophilization for 1 day.

Preparation of Two-Dye DMs with Different Surface Functional Groups: To prepare Cou6-encapsulated, RHO-labeled DMs (two-dye DMs), 2 mg of acetylated, RHO-labeled PDC synthesized according to our previous publication[25] was mixed with 10 mg of either unlabeled PDC-NH_2, PDC-Ac, or PDC-COOH in 1.2 mL DMF, and 2% (wt%) of Cou6 was added to the mixture. The materials were fully dissolved and mixed by brief vortexing followed by gentle stirring for 2 h. The two-dye DMs were prepared using the dialysis method, and the final products were obtained as powder after lyophilization as described above.

Characterization of the Prepared DMs and Liposomes Using Dynamic Light Scattering (DLS): Particle size (diameter, nm) and surface charge (zeta potential, mV) of the DMs and liposomes were measured from three repeat measurements by quasi-elastic light scattering using a Nicomp 380 Zeta Potential/Particle Sizer (Particle Sizing Systems, Santa Barbara, CA).[24,25] The materials were dispersed in ddH_2O to a concentration of 500 μg/mL and briefly vortexed prior to each measurement. The average value and standard deviation were calculated from 10 measurements.

In Vitro Drug Release Test: The drug release test was performed using a vertical Franz diffusion cell device (Φ7 mm with 0.38 cm^2 exposure area, PermeGear Inc., Hellertown, PA). A cellulose membrane (MWCO 3500) was sandwiched between the donor and receiver chambers. Various amounts of the micelles and liposomes, normalized to contain the same amount of EDX, were suspended in ddH_2O, and 100 μL of each solution was applied to each donor chamber. The receiver solution (release media), composed of 30% ethanol and 70% normal saline, was stirred constantly at 600 rpm, and the temperature was maintained at 37 °C. At predetermined time intervals, 250 μL of release media were removed and replaced with an equal amount of fresh receiver solution and analyzed using RP-HPLC (see SI for method descriptions). The release profile was obtained by plotting the cumulative EDX release% against time. The release rates were obtained from the slope of each steady release phase (linear portion) of the release curve. For the biphasic release profiles, the release rates of the first 8 h and day 1 to 6 were separately calculated.

In Vitro Anti-proliferation Assay of Breast Cancer Cell: The ER+ MCF-7 and the ER– MDA-MB-231 breast cancer cells (American Type Culture Collection, ATCC, Manassas, VA) were cultured according to the published protocol[42] and was described in SI. After the stripped cells were incubated in the phenol red-free medium with or without 0.1 nM of E2 overnight, 100 μL of stripped medium containing 0.1 nM of E2 with various concentrations of EDX (0, 10, 100, and 500 nM) and 0.01% DMSO (vehicle), EDX-loaded DMs with equivalent drug concentrations, or empty DMs with equivalent micelle concentrations were added to each well in 96-well plates (n = 3). The treatment was repeated every other day up to the twelfth day. The cell proliferation was assessed using a CellTiter 96 AQueous One Solution (MTS) Reagent (Promega Corp., Madison, WI) according to the manufacturer's protocol. Detailed descriptions can be found in the SI.

Preparation of Mouse and Human Skin Samples and Franz Diffusion Cell Experiments: The research use of hairless mice was approved by the Office of Animal Care and Institutional Biosafety Committee at the University of Illinois at Chicago (protocol number: 12–166). Full thickness mouse skin (average thickness 360 ± 20 μm, mean ± SD) was collected from the dorsal side of the 6–8 weeks old SKH1 hairless mice (Charles River Laboratory, Boston, MA).[43] Subcutaneous fat and blood vessels were carefully removed using cotton swabs. The research use of human skin samples was approved by the Institutional Review Board at the Northwestern University (protocol number CR4_STU00023488), and the skin permeation experiments were performed in the Khan laboratory. The split-thickness skin (STS) samples from two subjects were prepared and used as described in a previous study.[4] The thickness of the STS samples was 390 ± 30 μm (mean ± SD).

Undamaged skin was cut into 1.2 × 1.2 cm^2 squares, rinsed with normal saline, and sandwiched between the donor and receiver chambers of the Franz diffusion cells with the SC side facing upward.[11] The receiver chambers were filled with fresh normal saline containing 30% ethanol (v/v). After equilibration of the skin at 37 °C for 30 min, 100 μL of each formulation were applied to the donor chambers. For mouse skin permeation experiments, four EDX formulations in ddH_2O (DM-NH_2, DM-Ac, DM-COOH and liposomes containing same amount of drug) were compared with free EDX in ddH_2O containing 60% ethanol. For human skin permeation experiments, three formulations were compared: 1) EDX-loaded DM-COOH in ddH_2O (4 mg/mL); 2) EDX in phosphate buffer (PB, 2 mM KH_2PO_4, 4 mM Na_2HPO_4, pH 7.0) containing 60% of ethanol (v/v); and 3) EDX in 60% ethanol-PB solution with the supplementation of 0.5% (v/v) of oleic acid (OA) as used in previous study.[4] The donor chambers were covered with Parafilm to avoid evaporation. The first sample collection was performed at pre-determined time points up to 24 h by withdrawing 250 μL of the receiver solution from each sampling port and replacing with 250 μL of fresh receiver solution. All solutions were kept at 4 °C in dark before analysis.

CLSM Imaging of the Mouse Skin Treated with Two-dye Dendron Micelles: SKH-1 hairless mouse skin was exposed to the two-dye DMs with different surfaces for 24 h in the Franz cell setup. The skin area that was exposed to the treatment was carefully collected, rinsed twice with ddH_2O for 10 min, and embedded into cryomolds (Tissue-Tek, Sakura Finetek USA, Inc., Torrance, CA). Skin was cryosectioned into 80 μm-thick slices and placed on anti-frost glass slides. The slides were then treated with 10% neutral buffered formalin for 10 min at RT and rinsed with ddH_2O. The fixed skin samples were then mounted with antiphotobleaching mounting media with DAPI (Vector Laboratory Inc., Burlingame, CA) and covered with glass cover slips. The slides were visualized using a Zeiss LSM 510 Meta CLSM (Carl Zeiss, Germany). The 488 nm line of a 30 mW tunable argon laser was used for the excitation of Cou6, a 1 mW HeNe at 543 nm for RHO, and a 25 mW diode UV 405 nm laser for DAPI. Emissions were filtered at 505–530 nm, 565–595 nm and 420 nm for Cou6, RHO, and DAPI, respectively.

Measurements of Skin Permeation and Retention: After the Franz cell experiment, donor solutions were collected and kept at 4 °C in dark before analysis. Skin was also collected and thoroughly cleaned. The effective exposure area on the skin was cut and homogenized in a 1.5 mL centrifuge tube. DMSO was used as a drug extraction reagent. After 12 h of extraction, the samples were centrifuged at 10 000 rpm for 10 min, and the supernatants were collected for analysis. RP-HPLC was used to detect EDX from the receiver solutions, skin extracts, and donor solutions using the conditions described in the SI. The steady state drug permeation rate (or flux, J) was obtained from the slope of the linear portion of the skin permeation curve. The time needed to reach the steady state permeation (or lag time, t_{lag}), was obtained from the intercept of the steady state permeation curve on the horizontal axis (time). The permeability coefficient (K_p) was calculated using the equation $K_p = J/C_v$, where C_v is the concentration of EDX in the formulation (drug loading). The diffusion coefficient (D) was calculated using the equation $D = h^2/(6 \times t_{lag})$, where h is the skin thickness.[44] The enhancement ratio (ER) was determined using the equation $ER = J_{nanoparticle}/J_{ethanol}$, where $J_{nanoparticle}$ is the flux obtained from the liposome or DM groups and $J_{ethanol}$ is the flux obtained from the ethanol group.[45]

For two-dye DMs treated skin, the fluorescence intensity in the donor and receiver solutions as well as in the skin extracts were detected using a SoftMax Pro spectrofluorometer (Spectra MAX, Molecular Devices Inc., Sunnyvale, CA). For the detection of Cou6 and RHO, the excitation wavelengths were 444 nm and 555 nm, and the emission wavelengths were 510 nm and 590 nm, respectively.

Statistical Analysis: Data processing and statistical analysis were performed using GraphPad Prism 6 (GraphPad Software, Inc., La Jolla, CA) based on a one-way ANOVA followed by Tukey's post hoc test. Data were considered significant at $p < 0.05$.

Supporting Information

Supporting Information is available from the Wiley Online Library or from the author. It includes detailed descriptions for material characterization (including TEM and HPLC) and cell culture/MTS assay procedures, along with additional proliferation data and an H&E stained skin image.

Acknowledgements

This work has been supported by Susan G. Komen Foundation under the grant #KG100713 and the Technological Innovation R&D Program (grant #S2083505) funded by the Small and Medium Business Administration (SMBA) of Republic of Korea. YY was partially supported by Chancellor's Graduate Research Fellowship from the University of Illinois at Chicago (UIC). RMP acknowledges partial support from the American Foundation for Pharmaceutical Education (AFPE) and Dean's Scholarship from UIC. The authors also thank Suhair Sunoqrot for her assistance in confocal imaging.

Received: September 21, 2013
Revised: November 18, 2013
Published online: January 20, 2014

[1] X. Wu, J. R. Hawse, M. Subramaniam, M. P. Goetz, J. N. Ingle, T. C. Spelsberg, *Cancer Res.* **2009**, *69*, 1722–1727.
[2] M. P. Goetz, S. K. Knox, V. J. Suman, J. M. Rae, S. L. Safgren, M. M. Ames, D. W. Visscher, C. Reynolds, F. J. Couch, W. L. Lingle, R. M. Weinshilboum, E. G. B. Fritcher, A. M. Nibbe, Z. Desta, A. Nguyen, D. A. Flockhart, E. A. Perez, J. N. Ingle, *Breast Cancer Res. Treat.* **2007**, *101*, 133–121.
[3] J. M. Rae, *Clin. Pharmacol. Ther.* **2013**, *94*, 183–185.
[4] O. Lee, D. Ivancic, R. T. Chatterton Jr, A. W. Rademaker, S. A. Khan, *Breast Cancer Target Therapy* **2011**, *3*, 61–70.
[5] J. Gjerde, S. Gandini, A. Guerrieri-Gonzaga, L. L. Haugan Moi, V. Aristarco, G. Mellgren, A. Decensi, E. A. Lien, *Breast Cancer Res. Treat.* **2012**, *134*, 693–700.
[6] E. R. Port, L. L. Montgomery, A. S. Heerdt, P. I. Borgen, *Ann. Surg. Oncol.* **2001**, *8*, 580–585.
[7] R. Day, P. A. Ganz, J. P. Costantino, W. M. Cronin, D. L. Wickerham, B. Fisher, *J. Clin. Oncol.* **1999**, *17*, 2659–2669.
[8] P. Rouanet, G. Linares-Cruz, F. Dravet, S. Poujol, S. Gourgou, J. Simony-Lafontaine, J. Grenier, A. Kramar, J. Girault, E. Le Nestour, T. Maudelonde, *J. Clin. Oncol.* **2005**, *23*, 2980–2987.
[9] M. R. Prausnitz, S. Mitragotri, R. Langer, *Nat. Rev. Drug Discov.* **2004**, *3*, 115–124.
[10] C. S. Mah, J. Singh Kochhar, P. S. Ong, L. Kang, *Intel. J. Pharm.* **2013**, *441*, 433–440.
[11] Y. Yang, S. Sunoqrot, C. Stowell, J. Ji, C.-W. Lee, J. W. Kim, S. A. Khan, S. Hong, *Biomacromolecules* **2012**, *13*, 2154–2162.
[12] R. K. Subedi, S. Y. Oh, M. K. Chun, H. K. Choi, *Arch. Pharm. Res.* **2010**, *33*, 339–351.
[13] P. Karande, A. Jain, K. Ergun, V. Kispersky, S. Mitragotri, *Proc. Natl. Acad. Sci. USA* **2005**, *102*, 4688–4693.
[14] B. C. Finnin, T. M. Morgan, *J. Pharm. Sci.* **1999**, *88*, 955–958.
[15] R. O. Potts, R. H. Guy, *Pharm. Res.* **1992**, *9*, 663–669.
[16] E. O. Aranda, J. Esteve-Romero, M. Rambla-Alegre, J. Peris-Vicente, D. Bose, *Talanta* **2011**, *84*, 314–318.
[17] A. C. Williams, B. W. Barry, *Adv. Drug Deliv. Rev.* **2004**, *56*, 603–618.
[18] Y. C. Tong, T. Y. Yu, S. F. Chang, J. H. Liaw, *Mol. Pharm.* **2012**, *9*, 111–120.
[19] D. E. Poree, M. D. Giles, L. B. Lawson, J. He, S. M. Grayson, *Biomacromolecules* **2011**, *12*, 898–906.
[20] Y. G. Bachhav, K. Mondon, Y. N. Kalia, R. Gurny, M. Moller, *J. Control. Release* **2011**, *153*, 126–132.
[21] A. Spernath, A. Aserin, A. C. Sintov, N. Garti, *J. Colloid Interface Sci.* **2008**, *318*, 421–429.
[22] Y. Yang, J. Bugno, S. Hong, *Polym. Chem.* **2013**, *4*, 2651–2657.
[23] R. M. Pearson, S. Sunoqrot, H.-J. Hsu, J. W. Bae, S. Hong, *Ther. Deliv.* **2012**, *3*, 941–959.
[24] J. W. Bae, R. M. Pearson, N. Patra, S. Sunoqrot, L. Vukovic, P. Kral, S. Hong, *Chem. Commun.* **2011**, *47*, 10302–10304.
[25] R. M. Pearson, N. Patra, H.-J. Hsu, S. Uddin, P. Kral, S. Hong, *ACS Macro Lett.* **2013**, *2*, 77–81.
[26] K. Kajimoto, M. Yamamoto, M. Watanabe, K. Kigasawa, K. Kanamura, H. Harashima, K. Kogure, *Intl. J. Pharm.* **2011**, *403*, 57–65.
[27] J. A. Bouwstra, P. L. Honeywell-Nguyen, G. S. Gooris, M. Ponec, *Prog. Lipid Res.* **2003**, *42*, 1–36.
[28] W. Ä. T. Al-Jamal, K. Kostarelos, *Accounts Chem. Res.* **2011**, *44*, 1094–1104.
[29] M. L. Turco Liveri, M. Licciardi, L. Sciascia, G. Giammona, G. Cavallaro, *J. Phys. Chem. B* **2012**, *116*, 5037–5046.
[30] Y. Yang, C. Hua, C.-M. Dong, *Biomacromolecules* **2009**, *10*, 2310–2318.
[31] D. D. Verma, S. Verma, G. Blume, A. Fahr, *Intl. J. Pharm.* **2003**, *258*, 141–151.
[32] L. Barbosa-Barros, C. Barba, G. Rodriguez, M. Cocera, L. Coderch, C. Lopez-Iglesias, A. de la Maza, O. Lopez, *Mol. Pharm.* **2009**, *6*, 1237–1245.
[33] Z. V. Leonenko, E. Finot, H. Ma, T. E. S. Dahms, D. T. Cramb, *Biophys. J.* **2004**, *86*, 3783–3793.
[34] C. Gregor, *Adv. Drug Deliv. Rev.* **2004**, *56*, 675–711.
[35] W. A. G. Bruls, H. Slaper, J. C. Van Der Leun, L. Berrens, *Photochem. Photobiol.* **1984**, *40*, 485–494.
[36] V. P. Shah, C. C. Peck, R. L. Williams, *Pharmaceut. Skin Penetration Enhancement* **1993**, *19*, 417–427.
[37] E. Hendradi, Y. Obata, K. Isowa, T. Nagai, K. Takayama, *Biol. Pharm. Bull.* **2003**, *26*, 1739–1743.
[38] M. T. Sheu, S. Y. Chen, L. C. Chen, H. O. Ho, *J. Control. Release* **2003**, *88*, 355–368.
[39] S. Ghosh, S. Hornby, G. Grove, C. Zerwick, Y. Appa, D. Blankschtein, *J. Cosmest. Sci.* **2007**, *58*, 599–620.
[40] S. Ghosh, D. Blankschtein, *J. Cosmest. Sci.* **2008**, *58*, 229–244.
[41] S. Mitragotri, *J. Control. Release* **2003**, *86*, 69–92.
[42] E. Pozo-Guisado, A. Alvarez-Barrientos, S. Mulero-Navarro, B. Santiago-Josefat, P. M. Fernandez-Salguero, *Biochem. Pharmacol.* **2002**, *64*, 1375–1386.
[43] F. Benavides, T. M. Oberyszyn, A. M. VanBuskirk, V. E. Reeve, D. F. Kusewitt, *J. Dermatol. Sci.* **2009**, *53*, 10–18.
[44] V. V. K. Venuganti, O. P. Perumal, *Intl. J. Pharm.* **2008**, *361*, 230–238.
[45] H. R. Moghimi, A. Alinaghi, M. Erfan, *Intl. J. Pharm.* **2010**, *401*, 47–50.